ELECTROPHOTOLUMINESCENCE AND THE ELECTRICAL PROPERTIES OF THE PHOTOSYNTHETIC MEMBRANE

I. Initial Kinetics and the Charging Capacitance of the Membrane

DANIEL L. FARKAS, RAFI KORENSTEIN, AND SHMUEL MALKIN
Departments of Biochemistry and Membrane Research, The Weizmann Institute of Science, 76100 Rehovot, Israel

ABSTRACT Preilluminated chloroplast membranes, and particularly hypotonically swollen vesicles (blebs), give rise to a strong characteristic luminescence (electrophotoluminescence, EPL; Ellenson and Sauer, 1976, *Photochem. Photobiol.*, 23:113–123; Arnold and Azzi, 1971, *Photochem. Photobiol.*, 14:233–240) during the application of a strong external electric field. A detailed kinetic study of EPL was carried out and the initial kinetics from the field onset are reported here. The fast rise time (<0.2 μs) of the applied external electric field together with a high instrumental time resolution allowed the observation of a characteristic delay (lag time) between the field onset and the appearance of the induced emission. The lag time decreased with increase in the applied field strength and/or the conductivity of the suspension and is interpreted to be a consequence of (*a*) the necessity to reach a threshold electrical potential difference in the bleb membrane, below which no emission can be triggered, and (*b*) the finite time required to attain such a transmembranal field during the charging process of the membrane. A quantitative analysis, connecting the lag time, the controllable experimental parameters, and the membrane electrical characteristics is presented. Its verification was carried out in both size-selected and heterogeneous bleb populations. In the latter, experiments were consistent with the assumption that the lag time reflects the charging of the largest blebs. The results indicate (*a*) the possibility of directly measuring the specific membrane capacitance, yielding an estimate of $C_m = 1.2 \pm 0.3$ μF/cm² (the precision being particle size–homogeneity dependent); (*b*) A minimal transmembranal potential difference (of ~240 mV) is necessary to induce electrophotoluminescence; and (*c*) the lag duration depends on the time elapsed between the preillumination and the external field application. Correlated with the study of ionophore effects on the lag time, this suggests additivity of the light- and field-induced transmembrane potentials in attaining the threshold for emission.

INTRODUCTION

Delayed luminescence emission in photosynthetic systems is thought to result from the reversal of the light-induced charge separation (1, 2). It can be considerably enhanced by various methods (3, 4), of which an externally applied electric field is unique in several respects: (*a*) very fast onset and offset, allowing for monitoring of the emission kinetics with high time resolution; (*b*) intensity, duration, and profile controllable in a wide range; (*c*) spatial directionality and sense, and (*d*) chemical and physical nonalteration of the sample, enabling repetitive measurements. The electric field–induced emission, first reported by Arnold and Azzi (5) and known as electrophotoluminescence (EPL) (6) is very sensitive in both magnitude and kinetics to the experimental conditions, including photosynthesis-related variables (photosystem II activity, preillumination, presence of inhibitors), the applied electric field (intensity, polarity, kinetics) and the suspension medium (osmolarity, viscosity, electrical conductivity, pH and temperature). Moreover, it is dependent on the characteristics of the photosynthetic membrane, and critically sc on the latter's being topologically closed and relatively nonconducting. In view of all this, analysis of EPL conveys valuable structural and functional information on photosynthetic systems (6–10). However, a detailed analysis of the results is hamperd by the fact that although the basic principle of EPL emission is readily understood (5–7), its peculiar kinetic pattern is still described only in phenomenological terms, by interplay of the photosynthetic and electrical variables that control the emission (8, 10). The shape and size heterogeneity of the chloroplastic particles in the suspension further complicates the quantitative assessment of the latter.

In this work, we concentrate on the very initial kinetics of EPL: the lag phase between the onset of the external field and the rise of the emission. We suggest that it reflects a simple process: the charging of the membrane as a capacitor. From the study of this phase under different conditions, one can evaluate the membrane's specific capacitance, estimate the electrical requirements for EPL production, and connect between the light-induced and

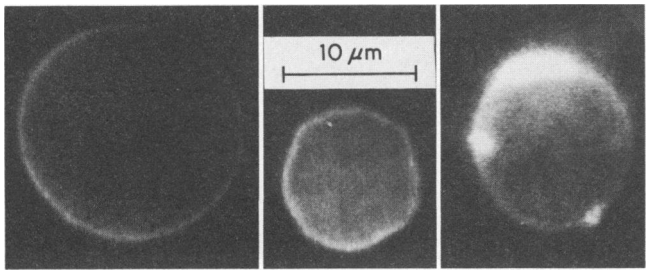

FIGURE 1 Typical bleb structures, produced by hypotonic swelling of pea thylakoids and viewed in an image-intensified fluorescence microscopy. The regions of very high brightness (*right*) correspond to "patches," piles of membraneous material.

electric field–induced transmembrane potentials. The analysis of the results is essentially unhindered by precursor depletion or electrical breakdown, whose influence is mainly felt at later stages of EPL.

METHODS

Chloroplasts from different sources, pea (*Pisum sativum*), lettuce (*Lactuca sativa*), tobacco (*Nicotiana tobacum, var. Xanthi*) and spinach (*Spinacea oleracea*), were prepared by a standard method (11) and stored below −100°C with complete preservation of essential photosynthetic activities (12). There were no species-dependent qualitative differences between them, and for a given set of experiments the same batch was used throughout. Blebs (13, 14) were generally preferred to thylakoids due to their spherical shape and larger size (Fig. 1). They were prepared by resuspending (usually 1:100) the stored chloroplasts in either distilled water or very dilute buffer (HEPES or Tricine, 5 mM, pH 7.8). Final chlorophyll concentrations were 10–40 μg/ml. The conductivity of the resulting suspensions was controlled by adding variable concentrations of KCl. The final specific conductivities were calculated from handbook data and checked with a conductometer (Metrohm AG, Herisau, Switzerland). The blebs showed photosystem II–related activity in giving rise to fluorescence induction (see reference 15) and electron transport from H_2O to dichlorophenolindophenol or ferricyanide. They were viewed and characterized by phase and image-intensified fluorescence microscopy (shape, Fig. 1 and size, Fig. 2). Use of a fluorescence-activated cell sorter (Beckton-Dickinson & Co., Paramus, NJ, Model FACS II) also allowed measurement of fluorescence and low-angle scattering of every individual particle in a suspension. We sought to improve the size distribution by simpler methods such as additional

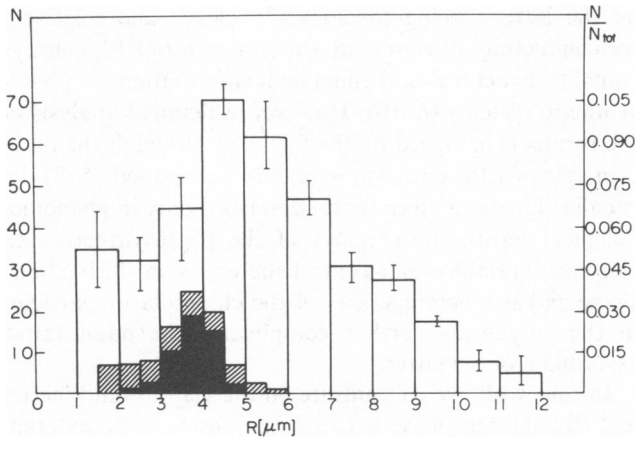

FIGURE 2 Size distribution of blebs, determined by use of an ocular with grating. Open areas, normal distribution; Hatched areas, size-selected population from the cell sorter (at regular flow velocities); Black areas, a better size selection (sorting at reduced flow velocity with a simultaneous choice of the low fluorescence ones).

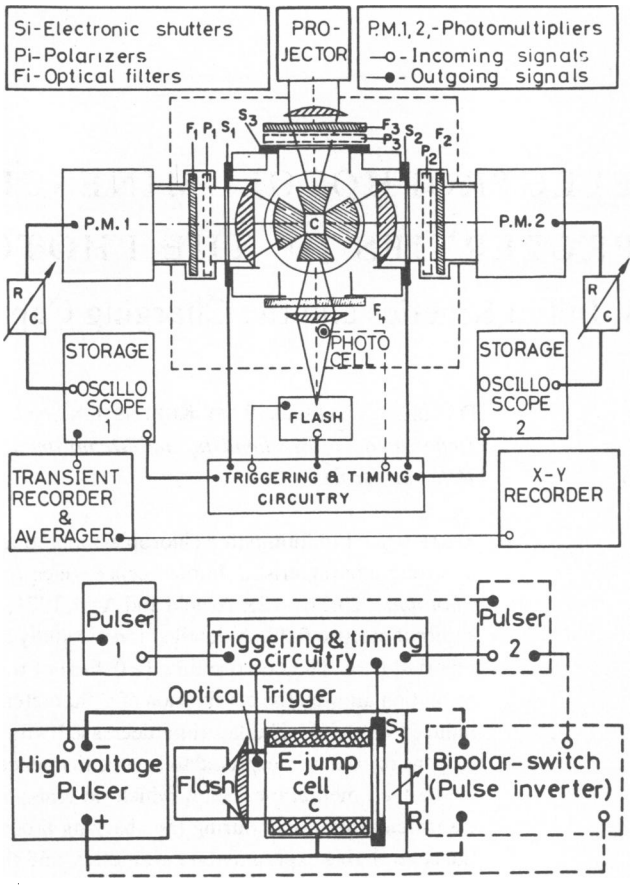

FIGURE 3 Experimental setup for electrophotoluminescence production and detection. *Bottom,* gross sketch of the electrical design for producing the applied field with the appropriate timing and kinetics in the *E*-jump cell (*C*). *Upper,* optical and monitoring portion of the instrumentation; the external field is applied to the cell (*C*) in a perpendicular direction to the plane of the drawing.

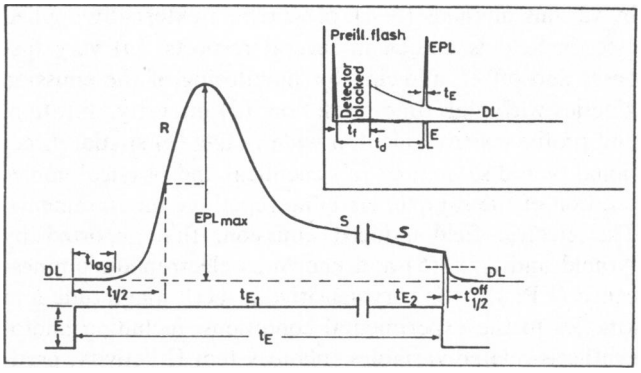

FIGURE 4 Schematic time course and parameters for electrophotoluminescence emission. *Inset,* time course of experimental events. Range of parameters for the figure given in Table I.

TABLE I
TYPICAL RANGE OF PARAMETERS FOR FIG. 4

$E = 100 \div 10{,}000$ V/cm	$t_f \sim 2 \div 10$ ms	$t_{1/2} \sim 3 \div 200$ μs	EPL/$DL = 1 \div 1{,}000$
$t_E = 1 \div 10{,}000$ μs	$t_d \sim 3 \div 10{,}000$ ms	$t_{1/2}^{off} \sim 10 \div 100$ μs	
$t_{E_1} \sim 1$ μs $\div 10^2$ μs	$t_{flash}^{1/2} \sim 10$ μs	$t_{lag} \sim 1 \div 40$ μs	
$t_{E_2} \sim 10^2 \div 10^4$ μs		$R/S \sim 0 \div 20$	

centrifugation (at 3,000 *g*), slower (dialysis controlled) hypotonic swelling, or by starting from intact instead of broken chloroplasts, but the advantages gained were marginal. However, in a particular set of experiments, we succeeded in selecting a bleb population of a definite radius, $R = 4 \pm 1$ μm (Fig. 2), by use of the cell sorter (see reference 16). We ensured that these blebs were also relatively devoid of "patches" (as in Fig. 1 *A*), by selecting low-fluorescence ones.

The apparatus for EPL production and detection is sketched in Fig. 3. Other details are given elsewhere (7, 8). The time resolution of both external field production and EPL detection was better than 0.2 μs, as checked directly. The typical time course and range of parameters for an experiment are shown in Fig. 4 and Table I. The lag time (t_{lag}) was estimated by monitoring the emission at high sensitivity (with its peak out of scale), allowing the relatively precise determination of the moment at which it exceeded the level of natural delayed luminescence. The light flash–induced carotenoid absorption changes were measured in an Aminco dual wavelength spectrophotometer Aminco, Silver Spring, MD, model DW2. The output of its photomultiplier was fed into a Nicolet 1170 digital oscilloscope and signal averager (Nicolet Instrument Corp., Madison, WI). All measurements were performed at 23°C.

RESULTS

Description of Electrophotoluminescence Emission

When, following preillumination (by either a short flash or continuous light), an external electric field pulse (typically 10^3 V/cm) was applied to a suspension of broken chloroplasts or blebs, a luminescence, stronger by one to three orders of magnitude than the natural delayed luminescence, was emitted (Fig. 5). The relatively complex kinetic pattern of this emission (EPL) is given schematically in Fig. 4, and includes most notably a rapidly rising and decaying component followed by a relatively slowing decreasing one, termed *R* and *S*, respectively (6, 8). Because the rise of the external electrical field was, in our work, extremely fast (<0.2 μs) the kinetic shape of the induced emission reflects the actual time-resolved response of the sample, quite unlike other stimulated luminescences (4). The existence of a lag phase (t_{lag} in Fig. 4) between the onset of the field and the rise of the emission is characteristic to all EPL. Its duration was typically a few microseconds, and was influenced by the experimental factors as follows: It was shortened as the intensity of the applied field increased (Fig. 6 A), in a dark time–dependent way (compare Figs. 6 *A* and 6 *B*), or by increasing the electrical conductivity of the medium (Fig. 6 *C*). It was lengthened by increasing the ionic permeability of the membrane, e.g., by gramicidin (Fig. 6 *D*) addition (8, 17). It was also, to a lesser extent, dependent on other experimental parameters like viscosity and osmolarity. (See Table III, below, for a

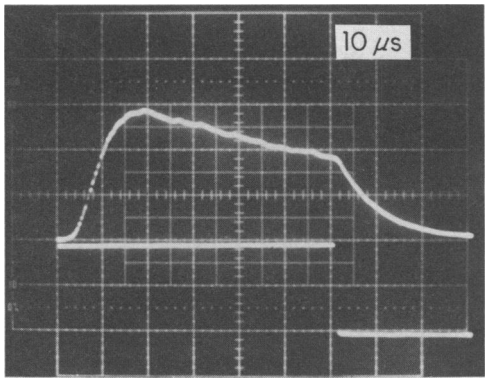

FIGURE 5 Electrophotoluminescence produced by a single DC electric field pulse. Lettuce chloroplasts resuspended and forced to form blebs in 5 mM Tricine buffer, pH = 7.8, 0.1 mM KCl, 296°K. $E = 1{,}500$ V/cm, $t_d =$ 200 ms. Both EPL (*top*) and the electric field (*bottom*) trace were monitored simultaneously. The lag in EPL emission is clearly visible. Time scale and sensitivity: 10 μs and 500 mV per division. (Under these conditions, a separate measurement of the natural delayed luminescence gave a value ~8 mV).

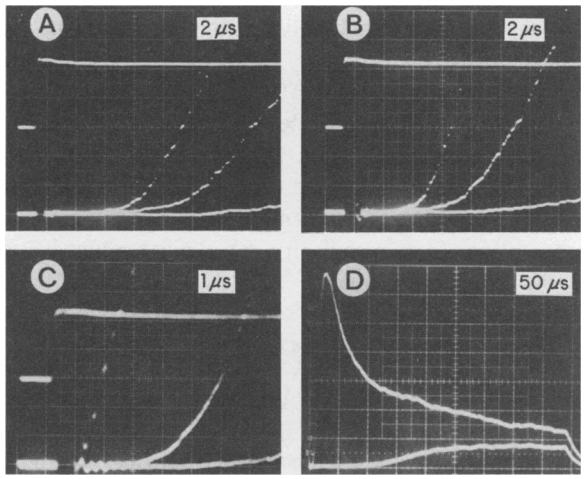

FIGURE 6 EPL traces showing the dependence of the lag time on experimental conditions from raw data. *Upper* trace in *A–C*: time course of the applied field (1,500 V/cm). *A, lower* traces (*bottom* to *top*): EPL emission for applied fields of 1,000 V/cm, 1,500 V/cm, and 2,000 V/cm, respectively. Conditions: 0.1 mM KCl, pH = 7.8, $t_d = 220$ ms. Sensitivity: 50 mV/division ($DL < 1$ mV under these conditions); *B*, the same as *A* but for $t_d = 70$ ms; *C*, the same as *A*, for an applied field of 1,500 V/cm, and for 0.1, 1, and 10 mM KCl, from *bottom* to *top*. *D*, upper trace: no additions. *Lower* trace: with 10 μM gramicidin D; $E = 1{,}500$ V/cm, 2 mM KCl, $t_d = 220$ m. Time scale as indicated.

summary of t_{lag} dependence on the field intensity and electrical conductivity.)

The Lag Phase and the Induced Transmembrane Electric Field

The above findings can be explained by assuming that the lag phase reflects the time needed to charge the vesicle (bleb) membrane to a certain minimal transmembranal potential difference, below which no electrophotoluminescence was detectable. Indeed, the factors listed above as influencing t_{lag} had a correlated influence on the emission itself (e.g., on EPL_{max}), because they all controlled the transmembranal electric field, both in its strength and kinetics. Thus, the higher the externally applied field, the stronger the membrane field is. The medium conductance reflects the availability of ions as current carriers for the transmembranal (local) field build up, and the viscosity influences their mobility; ionophores facilitate the transmembrane movement of ions, thus diminishing the local enhancement of the external field (17). On the other hand, a number of factors that influence EPL markedly have only a marginal influence on t_{lag}. These are mostly photosynthetic activity–related factors such as preillumination intensity and duration, temperature, presence of artificial electron donors or acceptors, or presence of inhibitors. These contrasting effects of the experimental conditions on the initial kinetics of EPL validate the concept that the main phenomenon reflected in the lag time is the electrical charging of the membrane. We suggest that a certain minimal membrane field value must be attained in the process of the electrical charging to observe EPL at all. This was confirmed not only by the total lack of field-induced emission during t_{lag} (as ascertained on a much more sensitive scale than that used in Fig. 5), but also by the experimental dependence of EPL on the externally applied field intensity (Fig. 7). Indeed, below a certain threshold applied field value (denoted E^*) no EPL emission occurred. For a given sample, E^* varied slightly with the conditions (e.g., osmolarity, t_d), typical values being in the 100–400 V/cm range.

A Quantitative Model

The description above can be expressed in quantitative terms as follows:

(*a*) The steady-state transmembranal field E_m induced in a spherical vesicle of radius R and membrane thickness d by an externally applied electric field E can be calculated by solving the Laplace equation for the electrostatic potential, with the appropriate boundary conditions at the interfaces separating between the external medium, the vesicle's membrane, and the inner medium, respectively. (The swollen thylakoid [bleb] can be considered as a spherical vesicle as is shown by phase- and image-intensified fluorescence in Fig. 1.) The most widely used

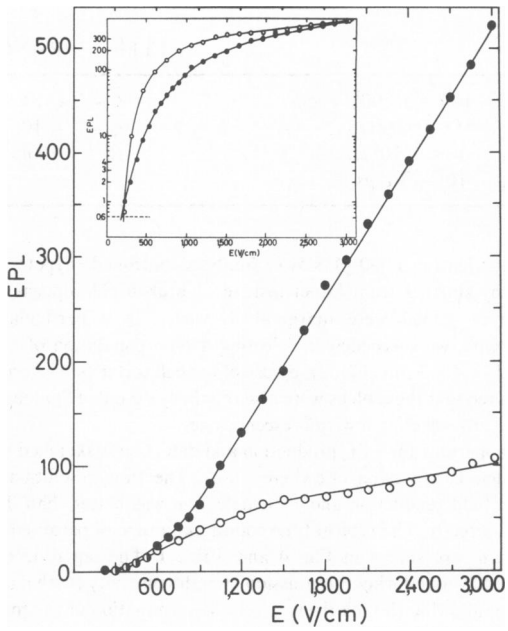

FIGURE 7 EPL peak intensity dependence on the external electric field intensity E. t_d = 22 ms (●), and t_d = 4,000 ms (○); 0.1 mM KCl, pH = 7.8. *Inset:* the same, plotted on a semilogarithmic scale. The readings for t_d = 4,000 ms (○) were multiplied by 5 for normalization; The dotted line (---) represents the value of naturally delayed luminescence (*DL*) at 22 ms.

expression (for examples see references 7, 10, 18) is

$$E_m = \tfrac{3}{2}(R/d)\, E \cos\theta \qquad (1)$$

where θ is the polar angle between the external electric field direction and the radius vector to the membranal plane, for any surface point. Eq. 1 is an approximate expression, obtained by assuming that $R \gg d$ and that the membrane electrical conductivity λ_m is negligibly low, compared with those of the external and internal media of the vesicle. More general formulae are given in references 6, 17, and 19 and the Appendix.

(*b*) The rise of the transmembrane field in a vesicle is not instantaneous, due to the finite capacitance of the membrane. The specific time course for the membranal field is derived in the Appendix. With the simple approximations used for Eq. 1, it is given by

$$E_m(t) = (3/2)(R/d)\, E \cos\theta \left[1 - \exp - \left(\frac{2\lambda_o\lambda_i}{2\lambda_o + \lambda_i}\frac{t}{RC_m}\right)\right]$$
$$= KE \cos\theta \left[1 - \exp - \frac{\gamma\lambda_o}{RC_m} t\right] \qquad (2)$$

where C_m is the specific membrane capacitance, K the field enhancement ratio and γ a numerical constant depending on the assumed ratio between the inner (λ_i) and outer (λ_o) medium specific conductivities.

The main assumption in the analysis is the existence of a certain critical membranal field value E_m^*, reflected in the

EPL vs. E plot by a corresponding critical external field E^* (Fig. 7), below which no emission of EPL is detectable. The plot of EPL vs. E on a semilogarithmic basis shows a very steep (orders of magnitude) decline below 500 V/cm (Fig. 7, inset); on a linear scale, this looks like a threshold in the field dependence. This definition of E^* is not very precise (±50 V/cm), and depends to a certain extent on the experimental noise level. If, instead of fast-rising DC field pulses, slowly rising (e.g., 50 Hz sinusoidal) external fields are used, a more precise determination of E^* is possible (see below).

During the charging of the membrane the membranal field increases from zero, attains the critical value E_m^*, and continues to increase to the steady state value. One can use Eq. 2 to calculate the lag time that is needed to reach E_m^*. The critical membranal field E_m^* will be attained first for the polar regions of the bleb (i.e., cos $\theta \sim 1$), and, for a given distribution of bleb sizes, for the largest R first (as $\partial E_m/\partial R > 0$ for any value of R, E, and t, as can be derived from Eq. 2). Application of different external fields (E) will result in different lag times for the appearance of EPL. The point in EPL kinetics where the emission starts to rise corresponds to $t = t_{lag}$ and $E_m = E_m^*$. Assuming that E_m^* (obtained when the membranal field is almost fully established) corresponds to E^* (i.e., the threshold external electric field that is required to observe EPL) in the relation of EPL and the external field given in Fig. 7, we obtain from Eq. 2 setting cos $\theta = 1$

$$t_{lag} = \frac{1}{\gamma\lambda_o} RC_m \ln \frac{E}{E - E^*}. \qquad (3)$$

From experimental measurements of t_{lag} vs E, analyzing the data according to Eq. 3, C_m can be evaluated directly. For this, the value of E^* is estimated from the EPL vs. E plots. With regard to the definition of R, the best approach would be to have a homogeneous population of blebs, of the same radius. However, heterogenous samples of a known distribution are much easier to obtain; for such samples R is defined as the largest radius of the distribution (see above).

Experiments on Size-selected Blebs. In a certain set of experiments, the blebs were selected by size, using the cell sorter (see Methods). The narrow size distribution of the resulting suspension is shown in Fig. 2 (black areas); it can be characterized by a radius $R = 4 \pm 1$ μm. The conductivity of the suspension was $\lambda_o = 2 \times 10^{-5}$ S/cm, and the minimal applied field to induce emission was found to be $E^* = 400$ V/cm. (One can calculate from this that [cf. Eq. 1] the corresponding threshold membrane potential [$E_m \cdot d$] is equal to ~240 mV). We measured the lag time for this sample, for different applied voltages, and plotted t_{lag} vs. ln [$E - E^*$)] as according to Eq. 3. As expected from Eq. 3, this dependence is indeed linear (Fig. 8) and allows the calculation of the specific capacitance C_m

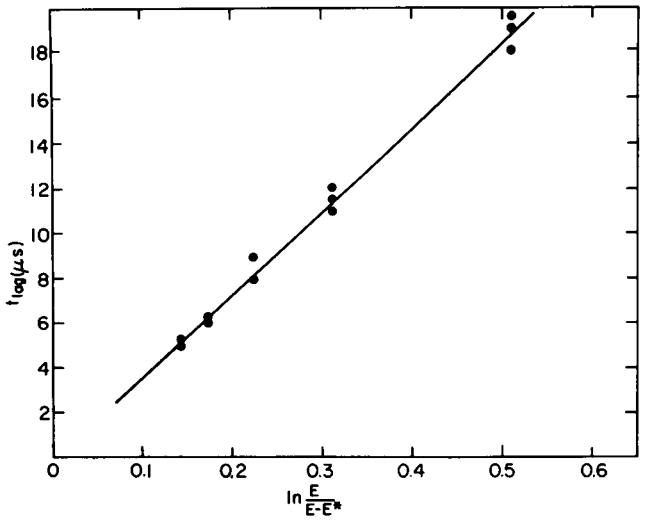

FIGURE 8 Externally applied field dependence of the lag time for size selected ($R = 4 \pm 1$ μm) blebs. $\lambda_o = 2 \times 10^{-5}$ S/cm, $t_d = 220$ ms. $E^* = 400$ V/cm (The value of E* was estimated from experiments on EPL vs. field). Every point represents the mean value of two measurements, and the different points stand for various alliquots from the same sample.

of the membrane:

$$C_m = \frac{2\lambda_o}{3R} S \qquad \text{(assuming } \lambda_i = \lambda_o\text{)} \qquad (4)$$

where S is the slope obtained from Fig. 8. It has been assumed that $\lambda_i = \lambda_o$, as the blebs were prepared directly in a medium having this conductivity. From Eq. 4, taking into account the errors in the measurement of the parameters that appear in it, we estimate that the membrane specific capacitance is $C_m = 1.2 \pm 0.3$ μF/cm^2.

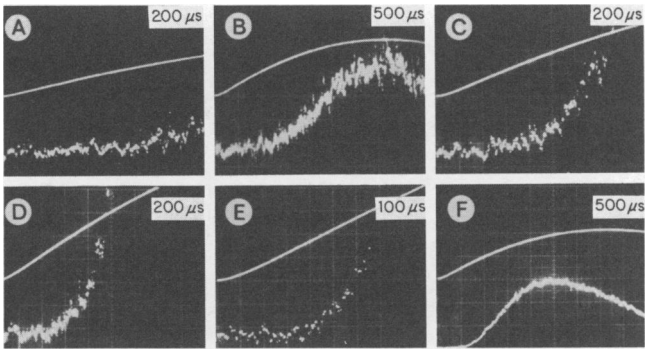

FIGURE 9 Electrophotoluminescence traces induced by slow-rising electric fields from blebs (10 μg chlorophyll/ml in 0.1 mM KCl pH 7.8 t_d = 300 ms). The slow field rise was achieved by combination of an AC signal generator and an amplifier, producing sinusoidal fields. In these experiments, the time course of the field was the same (AC frequency 36 Hz) but its peak (E_{peak}) value varied at will: *A* (240), *B* (240), *C* (460), *D* (470), *E* (1,070), *F* (1,070) V/cm, respectively. *Upper* trace, time course of the external field (scale: in *A–E* ~100 V/cm per division; in *F* ~500 V/cm per division; base line in the middle). *Lower* trace, EPL kinetics (scale: A–E 20 mV/division; *F* [25 times less sensitive], 500 mV/division). Time scale as indicated.

TABLE II
VALUES OF THRESHOLD CRITICAL ELECTRIC FIELD, E^*, FOR EPL EMISSION IN DIFFERENT RISING FIELDS. SOME CHOSEN EXAMPLES

Initial rate of field increase (V/cm · ms)	54*	125‡	201‡	242*	298‡
E* (V/cm)	126	133	135	140	140

AC frequency 36 Hz* and 50 Hz‡; various E_{peak}

Heterogenous Distribution of Bleb Sizes

As the availability of the cell sorter apparatus was limited, and the selection process slow, we continued this investigation on samples with relatively broad spectra of bleb radii (e.g., Fig. 2). The basic observation of a lag period and the necessity of a threshold field were still reproduced. The requirement for a certain critical field was further confirmed in experiments where the rise of the applied field is much slower than the presumed membrane charging rate, so that the membranal field is practically proportional at any moment to the external field.

A set of such experiments is shown in Fig. 9. The applied fields increased quasi-linearly, with rates ranging between 100 and 400 V/cm per ms. Although EPL intensities depended strongly on the rate of increase, the critical field E^* value obtained, below which EPL was undetectable was the same (~135 V/cm) for all voltage increase regimes (Fig. 9 and Table II). Although this estimate of E^* seems lower than that obtained with the size-selected particles, one must consider that here the suspension also contained blebs having much larger radii, which attain the critical membranal E_m^* field at lower applied external fields. In fact, the threshold values for lag and field must correspond to the largest particles in the given distribution. In view of this, the calculated threshold transmembranal potential (E_m) (estimated by use of Eq. 1 for a bleb with $R = 12\ \mu m$; see Fig. 2) was found to be ~240 mV, which is the same as for the size-selected particles.

Turning to the case of fast-rising fields we checked Eq. 3 again by calculating $\ln [E/(E - E^*)]$ for various measured values of t_{lag} using $E^* = 135$ V/cm. This was repeated in different experiments varying λ_o for each experimental series by a suitable addition of salt to the medium (Table III). The ratio of t_{lag} to $\ln [E/(E - E^*)]$ for each experimental series is fairly constant as predicted

TABLE III
LAG-TIME DATA FOR A HETEROGENOUS POPULATION OF BLEBS AT VARIOUS OUTER MEDIUM CONDUCTIVITIES (λ_o) AND DIFFERENT APPLIED FIELDS (E)

λ_o	E	t_{lag}	$\ln \frac{E}{E - E^*}$	$10^6 \frac{t_{lag}}{\ln E/(E - E^*)}$		λ_i	C
10^5 s/cm	V/cm	μs				10^5 s/cm	μF/cm²
2	1,850	9.0	0.076	118			
	1,450	10.5	0.098	107	Average	2	1.04 ± 0.13
(initial medium)	1,200	11.5	0.119	97	94 ± 12		
	900	14.0	0.162	86			
	600	22.0	0.254	87			
	480	30.0	0.33	91			
10	1,850	4.0	0.076	53			
	1,450	5.0	0.098	51	Average	3.2	
	1,200	5.5	0.119	46	45 ± 6		
	900	7.0	0.163	43			
	600	11.5	0.254	45			
	480	14.0	0.33	42			
20	1,850	3.5	0.076	46			
	1,450	4.0	0.098	41	Average	3.4	
	1,200	5.0	0.119	42	39 ± 3		
	900	6.0	0.163	37			
	600	9.5	0.254	37			
	480	12.0	0.33	36			
40	1,850	3.0	0.076	39			
	1,450	3.5	0.098	36	Average	4.0	
	1,200	4.0	0.119	34	33 ± 3		
	900	5.5	0.163	34			
	600	8.5	0.254	33			
	480	10.0	0.33	30			

Membrane-specific capacitance (C_m) was calculated (Eq. 3) for the initial medium conductivity, assuming $\lambda_i = \lambda_o$. Inner phase conductivities (λ_i) were calculated assuming the same membrane specific capacitance ($C_m = 1.04\ \mu F/cm^2$). E^* was taken from the data of Table I (135 V/cm). R was taken as the largest bleb size (12 μm). As E increases the error in $\ln[E/(E - E^*)]$ due to any error in E^* increases greatly. Therefore the value for $E = 1{,}850$ was not included in the averaging.

from Eq. 3. The calculated value of C_m for the initial (low conductivity) medium assuming $\lambda_i = \lambda_o$ gives a value for C_m (1.04 ± 0.13 μF/cm^2) fairly close to the value obtained for size-selected blebs. However, the data of the other higher λ_o experimental series are not consistent with $\lambda_i = \lambda_o$: The ratio t_{lag} to ln $[E/(E - E^*)]$ does not decrease as much as would be expected from the increase in the outer medium conductivity (Table III). Therefore, we have to assume that there is no full equilibration of the outer and inner media with respect to the added salt concentration. Assuming C_m to remain the same, as for the medium where the blebs were prepared, we calculated λ_i, using Eq. 3 (Table III). The results show indeed a very modest increase in λ_i as λ_o increases. These findings underline the importance of using for estimation of C_m, a low salt concentration medium such as that used to prepare the blebs, for which $\lambda_i = \lambda_o$.

Although the heterogenous population of blebs gave results similar to the size-selected ones, we regard the latter as more precise, in view of the uncertainty in R.

The Lag Time and the Photosynthetic Light-induced Membrane Potential

For a given bleb size distribution and applied field intensity, the length of the lag time depends on the dark time, t_d (see Fig. 4 inset), elapsing between the preillumination flash and the application of the external electric field (compare Figs. 6 *A* and 6 *B*). The differences are particularly important in the first tens of milliseconds following the flash (Fig. 10 *B*). Two parameters of the system undergo a considerable change in this range, namely the availability of precursors (which decreases with a second-order kinetics in the dark [6, 7], and the light-induced transmembrane electrical potential (Fig. 10 *A*), the decay of which can be monitored by the carotenoid electrochromic shift (20). As the availability of precursors does not influence t_{lag}, the striking similarity (mirror symmetry) between the dark-time dependence of the carotenoid shift and that of t_{lag}, respectively (Fig. 10) leads to the assumption of the light-induced potential being responsible for the change in t_{lag}. This could be explained as follows: If the external field and light-induced potentials were additive, and a threshold potential is needed for EPL to occur (e.g., ~240 mV as discussed above), the externally applied field should contribute different proportion of this potential at different dark times. For a constant applied voltage, this would manifest itself in different lag times, increasing with increase of t_d.

To further establish this view, we used ionophores such as valinomycin and gramicidin to affect the light-induced field. Their action on the light-induced carotenoid shift is illustrated in Fig. 10 *A*. Valinomycin, being a carrier type ionophore, accelerates the decay of the light-induced potential, but does not affect its rise. Gramicidin, on the other hand, being a channel-type ionophore, almost totally

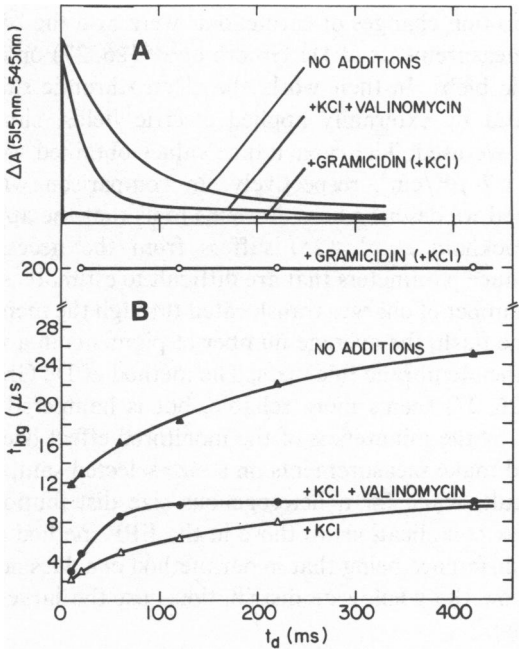

FIGURE 10 Decay of the light-induced carotenoid electrochronic spectral shift (*A*) and dark-time (t_d) dependence of EPL lag time (*B*). Applied field intensity of E = 1,000 V/cm. Initial suspension (no addition) medium contained 0.1 mM KCl. Additions were 2 mM KCl, 5 μM valinomycin, and 10 μM gramicidin D, as indicated. The *top* curves were obtained after averaging and smoothing of the response to a 10-μs saturating flash, while t_{lag} for various dark times was measured directly.

collapses the light-induced potential. These ionophores affect EPL emission itself (see Fig. 6 *D* and reference 17), but we concentrate here on their action on the lag phase only. As shown in Fig. 10, in the presence of valinomycin t_{lag} vs. t_d is almost a mirror image of the light-induced potential decay in the presence of the same ionophore, in spite of the change of kinetics. In the presence of gramicidin, the lag time is severely lengthened as the membrane conductivity increases considerably, requiring, therefore, much longer time to achieve the threshold potential. This lag time is not influenced at all by t_d, in consistence with the total absence of the light-induced potential.

DISCUSSION

The Membrane Capacitance

Our estimate of the membrane specific capacitance (C_m = 1.2 ± 0.3 μF/cm^2) agrees well with values usually obtained for natural membranes (21, 22). As pointed out by Cole (23), practically all the values obtained for membrane capacitances range between 0.6 and 2.0 μF/cm^2. Therefore, we view the result mostly as a confirmation of the approach. It should be stressed, however, that there are relatively few direct measurements of the photosynthetic membrane capacitance in the literature (24). Recently, Packham et al. (25) measured the charging capacitance of the chromatophore membrane, obtaining a value of 1.1 μF/cm^2, by analysis of the light-induced carotenoid shift.

Absorption changes of carotenoids were also the basis for the measurements of De Grooth et al. (26, 27) on chloroplastic blebs. In their work, the electrochromic shift was induced by externally applied electric fields, similar to those we used. The capacitance values obtained were 2.0 and 1.7 $\mu F/cm^2$, respectively. In comparison with the method we describe here, it seems to us that the approach of Packham et al. (25) suffers from the necessity to introduce parameters that are difficult to estimate, such as the number of charges translocated through the membrane by one flash, the average number of pigments in a vesicle, and the membrane thickness. The method of De Grooth et al. (26, 27) seems more reliable, but is hampered somewhat by the minuteness of the monitored effect itself; this would make measurements on a size-selected sample very difficult, while for a heterogenous size distribution very similar complications to those in the EPL method appear (the difference being that in our method one does not have to know the whole size distribution, just the largest bleb radius).

Having justified the validity of our approach, the main improvements needed to arrive at a more accurate estimation of the membrane electrical parameters are (*a*) achieving size homogeneity of the sample, (*b*) a more precise procedure to find the lag in EPL vs. t and EPL vs. E, and (*c*) a clear separation between the two components of EPL, the rapid and slow emission, each with its own dependency on E.

EPL vs. the Electric Field Strength

Our results indicate different dependence of EPL vs. the electric field strength than is customary [6, 10] to assume. Usually it was thought that EPL manifests a direct increase of the recombination rate, and that the increase of this rate is due to lowering of the activation energy by a term proportional to E_m that leads to an exponential factor $\exp(E_m/kT)$ in the expression for the rate of recombination. From the polar-angle, θ, and external field dependence (Eq. 1) integration over the whole sphere leads, in this model, to luminescence proportional to $\cosh(E/kT)$, approximated by an exponential when EPL is much higher than ordinary delayed luminescence. Such a concept does not really lead to our observations of a threshold voltage and a lag time in the EPL kinetics. The results in Fig. 7 (inset) particularly show that above a certain threshold, EPL increases over a narrow range of field intensities by more than two orders of magnitude, but it then increases very moderately as the field increases further. This is in contrast to an exponential dependence.

Moreover, not only the maximal EPL, but also the total integrated luminescence increases with the field. This hints to the fact that there are two recombinational routes, radiative and nonradiative, and that both the rate and yield of the radiative route increase with the field (however, see reference 10). Thus, the present theory (5, 6, 10, 28) is too naive to explain these experimental facts.

Without going presently to any new concept, if one assumes monotonous dependence of EPL vs. E_m over a positive range of E_m (i.e., when directed from the inside to the outside of the membrane bleb) and no EPL for negative values of E_m, the threshold could indicate the presence of permanent negative (static) field that must be added to the induced field. Only when the sum of the two fields reaches above zero does EPL result. The effect of the photo-induced potential on the lag time, which supports such additivity of fields, is also in accord with such a concept. The threshold field cannot be very sharp experimentally because of the polar-angle, θ, dependence and the wide size distribution.

Electrophotoluminescence as a Probe of Membrane Properties

The external electric field–induced luminescence (EPL) from photosynthetic (thylakoid) membranes can be regarded as an intrinsic, fast-responding, voltage-sensitive probe yielding information on membrane structure and function. Some of the results obtained already in this direction include (*a*) pigment orientation at the reaction center of photosystem II, studied by EPL emission polarization due to electroselection in the membrane by the angular dependence of the induced field (7) and (*b*) the kinetics, effectiveness, and intercationic selectivity of ion translocation by ionophores (17), monitored by the changes induced in EPL due to the latter's extreme sensitivity to membrane electrical conductivity (see Eq. A30 and Fig. 6 *D*). More generally, basic features of the interaction between an external electric field and a vesicular membrane system can be studied by electrophotoluminescence. The investigation presented here has been devoted to the initial kinetics of this interaction, by making use of the fast rise time, or the variable profile of the applied field. A study of dielectric breakdown and recovery, using a succession of field pulses of reversed polarities and the opposite field action on the two bleb hemispheres, will be presented elsewhere.

APPENDIX

Let us consider the chloroplastic bleb as a microscopic, spherical particle of radius R, bounded by a single dielectric shell (the membrane) of thickness d (Fig. 11). Let us calculate the intensity and time course of the electric field induced in the membrane by an externally applied electric field of intensity E.

The electrostatic potential U obeys the Laplace equation

$$\Delta U = 0. \qquad \text{(A1)}$$

We will choose a system of spherical coordinates (r, θ, ϕ) having its origin at the center of the particle, and the $0z$ axis parallel to the direction of the applied field E. In these spherical coordinates, after separation of variables and taking into account the symmetry relative to the polar axis $0z$, the general solution of Eq. A1 can be expressed in the following

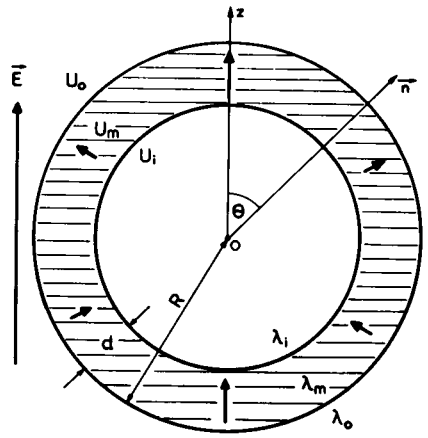

FIGURE 11 Model for a spherical membrane-bound particle in an external electric field: E, the externally applied electric field; θ, angle between the field direction and the normal to the plane of the membrane, at a certain point; U, electrostatic potential; λ_o, λ_i, λ_m specific electrical conductivity; R, radius of the vesicle; d, membrane thickness. Subscripts o, i, and m stand for the outer, inner, and membrane phases, respectively. Thick arrows within the membrane indicate the direction and angular dependence of the intramembrane field intensity (E_m).

form:

$$U(r, \theta) = \Sigma_n \left[A_n r^n + \frac{B_n}{r^{n+1}} \right] P_n(\cos\theta) \qquad \text{(A2)}$$

where $P_n(\cos\theta)$ are the Legendre polynomials. Limitation of Eq. A2 to one term ($n = 1$) gives a solution that is still general enough to meet the boundary conditions, and therefore should also represent the unique solution. Division of the space into three regions, namely, the outer (subscript o), inner (subscript i), and the membrane (subscript m) leads then to the solution

$$U_j(r, \theta) = A_j r \cos\theta + \frac{B_j}{r^2}\cos\theta \qquad (j = o, i, m, \text{respectively}). \qquad \text{(A3)}$$

Here A_j and B_j are six coefficients to be determined. We will assume them to be time dependent, as we are interested in the time course of the potential difference. The six conditions necessary for finding the coefficients will be given by the following:

(*a*) The continuity of the potential at the boundaries separating the regions, i.e.

$$U_i(r = R - d, \theta) = U_m(r = R - d, \theta) \qquad \text{(A4)}$$

$$U_m(r = R, \theta) = U_o(r = R, \theta). \qquad \text{(A5)}$$

(*b*) The finiteness of the potential everywhere, including the origin, yielding

$$B_i(r = 0, \theta) = 0, \qquad \text{i.e., } B_i = 0. \qquad \text{(A6)}$$

(*c*) The nonperturbation of the external field by the particle, at large distances, giving

$$E = -\frac{\partial U_o}{\partial(r\cos\theta)} = -A_o. \qquad \text{(A7)}$$

(*d*) The conditions related to charge movement and accumulation at the membrane surface. These are obtained by taking the time derivatives of the equation expressing the dependence of the discontinuity of the displacement vectors ($E = \epsilon E$) normal to the surface, on the surface charge densites, σ_j (i.e., $\delta[\epsilon E] = 4\pi\sigma_j$), and equating the rate of the surface charge density change with the radial currents at the surface. The currents are expressed with the aid of the specific ion conductivities λ_j and the radial field $E_r = (-\partial U/\partial r)$. One obtains

$$\epsilon_m \frac{dE_{mr}}{dt} - \epsilon_i \frac{dE_{ir}}{dt} = 4\pi \frac{d\sigma_i}{dt} = 4\pi \left\{ -\lambda_i A_i \cos\theta + \lambda_m \left[A_m - \frac{2B_m}{(R-d)^3} \right] \cos\theta \right\} \qquad \text{(A8)}$$

$$\epsilon_o \frac{dE_{or}}{dt} - \epsilon_m \frac{dE_{mr}}{dt} = 4\pi \frac{d\sigma_o}{dt} = 4\pi \left\{ \lambda_o \left[-E - \frac{2B_o}{R^3} \right] - \lambda_m \left[A_m - \frac{2B_m}{R^3} \right] \right\} \cos\theta \qquad \text{(A9)}$$

where Eqs. A6 and A7 have already been taken into account. Expressing A_i and B_o in Eqs. A8 and A9 from Eqs. A4 and A5, setting

$$\epsilon_o = \epsilon_i \equiv \epsilon \qquad \text{(A10)}$$

and considering

$$(R - d)^3 \simeq R^3 - 3R^2 d \qquad \text{(as typically } R/d \simeq 1{,}000 \text{ for blebs)} \qquad \text{(A11)}$$

we obtain by substitution in Eqs. A8 and A9 and rearrangement:

$$(2\epsilon + \epsilon_m)\frac{dA}{dt} + 2(\epsilon - \epsilon_m)\frac{dB}{dt} + 4\pi(2\lambda_o + \lambda_m)A + 4\pi(2\lambda_o - 2\lambda_m)B + 12\pi\lambda_o R^3 E = 0 \qquad \text{(A12)}$$

and

$$(\epsilon - \epsilon_m)\left(1 - \frac{3d}{R}\right)\frac{dA}{dt} + (\epsilon + 2\epsilon_m)\frac{dB}{dt} + 4\pi(\lambda_i - \lambda_m)\left(1 - \frac{3d}{R}\right)A + 4\pi(\lambda_i + 2\lambda_m)B = 0. \qquad \text{(A13)}$$

Here we substituted

$$R^3 A_m = A \qquad \text{(A14)}$$

$$B_m = B \qquad \text{(A15)}$$

$$E_{jr} = -\frac{dU_{jr}}{dr} = \left(-A_j + \frac{2B_j}{r^3} \right)\cos\theta. \qquad \text{(A16)}$$

Let us assume that $\lambda_m \ll (\lambda_i, \lambda_o)$ as is usually the case. To solve for $A = A(t)$ and $B = B(t)$, we will write for them the general form of a solution for the above system of first-order differential equations with constant coefficients:

$$A = A_0 + A_1 e^{-\alpha_1 t} + A_2 e^{-\alpha_2 t} \qquad \text{(A17)}$$

$$B = B_0 + B_1 e^{-\alpha_1 t} + B_2 e^{-\alpha_2 t}. \qquad \text{(A18)}$$

Substitution of Eqs. A17 and A18 into Eqs. A12 and A13 leads to the following homogeneous algebric equations for either the unknowns A_1, B_1,

or A_2, B_2:

$$[8\pi\lambda_0 - (2\epsilon + \epsilon_m)\alpha_k]A_k + [8\pi\lambda_0 - 2(\epsilon - \epsilon_m)\alpha_k]B_k = 0$$

$$\left[4\pi\lambda_i\left(1 - \frac{3d}{R}\right) - (\epsilon - \epsilon_m)\left(1 - \frac{3d}{R}\right)\alpha_k\right] \cdot A_k + [4\pi\lambda_i - (\epsilon + 2\epsilon_m)\alpha_k]B_k = 0 \qquad k = 1.2. \quad \text{(A19)}$$

The solution are nonzero, providing that the determinant of the coefficients is zero. This condition will set the solutions for α_1 and α_2. From this the following quadratic equation for α_i ($i = 1, 2$) is obtained:

$$\left[9\epsilon\epsilon_m + \frac{6d}{R}(\epsilon - \epsilon_m)\right]\alpha_k^2 - \left[3\epsilon_m(8\pi\lambda_0 + 4\pi\lambda_i) + \frac{6d}{R}(\epsilon - \epsilon_m)(4\pi\lambda_0 + 4\pi\lambda_i)\right]\alpha_k + 96\pi^2\lambda_0\lambda_i\frac{d}{R} = 0 \quad \text{(A20)}$$

written briefly as $M\alpha^2 + N\alpha + P = 0$. We will consider the orders of magnitude of the coefficients appearing in Eq. A20, to make a reasonable approximation for α_1 and α_2. Setting $d/R = 0$ (i.e., $P = 0$) gives the approximation limits, which are $\alpha_1 = 0$ and $\alpha_2 = -N/M$. Considering P finite but still small compared with $N^2/4M$, one will obtain α_1 as a small quantity approximated by $-P/N$ while α_2 is still fairly closed to $-N/M$. Thus

$$\alpha_1 \simeq \frac{4\pi d}{\epsilon_m R} \cdot \frac{2\lambda_0\lambda_i}{2\lambda_0 + \lambda_i} = \frac{1}{RC_m}\frac{2\lambda_0\lambda_i}{2\lambda_0 + \lambda_i} \quad \text{(A21)}$$

and

$$\alpha_2 = \frac{4\pi}{3\epsilon}(2\lambda_0 + \lambda_i). \quad \text{(A22)}$$

In Eqs. A21 and A22, M and N were approximated by dropping the terms containing d/R. This is justified since $d/R \sim 1/1{,}000$, while $\epsilon/\epsilon_m \sim 40$.

To find A_k, B_k ($k = 0, 1, 2$) we identify the coefficients of the exponentials after introducing Eqs. A17 and A18 into Eqs. A12 and A13. We obtain, again dropping terms in d/R,

$$A_0 = -A_1 = A_2 = -B_0 = B_1 = 2B_2 = -\frac{R^4E}{2d}. \quad \text{(A23)}$$

With these, and α_1 and α_2 from Eqs. A21 and A22, we get

$$E_m = \left(-A_m + \frac{2B_m}{R^3}\right)\cos\theta = E_m^{max}\cos\theta \cdot \left[1 - \exp\left(-\frac{2\lambda_0\lambda_i t}{(2\lambda_0 + \lambda_i)RC_m}\right)\right] \quad \text{(A24)}$$

with

$$E_m^{max} = 1.5\,(R/d)E. \quad \text{(A25)}$$

Eq. A24 has been obtained with the simplifying assumptions $d \ll R$ and $\lambda_m \ll \lambda_i, \lambda_0$. Without these assumptions, a more general expression can be obtained. Let us calculate E_m^{max} for the general case. For the steady state, Eqs. A8 and A9 can be replaced by

$$\lambda_i\frac{\partial U_i}{\partial r}(r = R - d) = \lambda_m\frac{\partial U_m}{\partial r}(r = R - d) \quad \text{(A26)}$$

and

$$\lambda_m\frac{\partial U_m}{\partial r}(r = R) = \lambda_0\frac{\partial U_0}{\partial r}(r = R). \quad \text{(A27)}$$

With the other four conditions (Eqs. A4 to A7), these lead, after some algebra, to

$$E_m^{max} = \frac{9\lambda_0\lambda_i E}{(2\lambda_0 + \lambda_m)(2\lambda_m + \lambda_i) - (2\lambda_0 - \lambda_m)(\lambda_i - \lambda_m)[(R - d)^3/R^3]} \quad \text{(A28)}$$

For specific cases Eq. A28 can be simplified. Thus, for $\lambda_0 = \lambda_i \gg \lambda_0$, it becomes

$$E_m^{max} = (9/2)\frac{E}{1 - (R - d)^3/R^3} \quad \text{(A29)}$$

i.e., the same as in reference 6. Of course with $R \gg d$, Eq. A29 reduces to Eq. A25 as in references (10, 18, 26). On the other hand, if $R \gg d$, but $\lambda_0 \neq \lambda_i$, and λ_m is not neglected Eq. A28 becomes

$$E_m^{max} = \frac{(3/2)(R/d)E}{1 + \frac{2\lambda_0 + \lambda_i}{2\lambda_0\lambda_i}\lambda_m(R/D)} \quad \text{(A30)}$$

which again reduces to Eq. A25 for $\lambda_m \ll (\lambda_0, \lambda_i)$.

This work was partly supported by the United States–Israel Binational Science Foundation, Jerusalem, Israel.

Received for publication 22 June 1982.

REFERENCES

1. Lavorel, J. 1975. Luminescence. *In* Bioenergetics of Photosynthesis. Govindjee, editor. Academic Press, Inc., New York. 223–317.
2. Malkin, S. 1977. Delayed luminescence. *In* Photosynthesis. I. Encyclopedia of Plant Physiology New Series. A. Trebst and M. Avron, editors. Springer-Verlag, Berlin. 5:473–491.
3. Fleischman, D. E., and B. C. Mayne. 1973. Chemically and physically induced luminescence as a probe of photosynthetic mechanisms. *Curr. Top. Bioenerg.* 5:77–105.
4. Malkin, S. 1977. Delayed luminescence. *In* Primary Processes of Photosynthesis. J. Barber, editor. Elsevier/North Holland Biomedical Press, Amsterdam. 351–431.
5. Arnold, W., and J. Azzi. 1971. The mechanism of delayed light production by photosynthetic organisms and a new effect of electric fields on chloroplasts. *Photochem. Photobiol.* 14:233–240.
6. Ellenson, J. L., and K. Sauer. 1976. The electrophotoluminescence of chloroplasts. *Photochem. Photobiol.* 23:113–123.
7. Farkas, D. L., R. Korenstein, and S. Malkin. 1980. Electroselection in the photosynthetic membrane: polarized luminescence induced by an external electric field. *FEBS (Fed. Eur. Biochem. Soc.) Lett.* 120:236–242.
8. Farkas, D. L., R. Korenstein, and S. Malkin. 1981. External electric field induced delayed luminescence in the photosynthetic membrane. *In* Photosynthesis I. Photophysical Processes, Membrane Energization. G. Akoyunoglou, editor, Balaban Intern. Sci. Services, Philadelphia 627–636.
9. Babcock, G. T., C. T. Yerkes, and W. J. Buttner. 1981. Static and dynamic electrostatic phenomena in chloroplast photosystem II.

Photosynthesis I. Photophysical processes, Membrane energization. G. Akoyunoglou, editor, Balaban Intern. Sci. Services, Philadelphia 637–645.
10. De Grooth, B. G., and H. J. van Gorkom. 1981. External electric field effects on prompt and delayed fluorescence in chloroplasts. *Biochim. Biophys. Acta.* 635:445–456.
11. Avron, M. 1960. Photophosphorylation by swiss-chard chloroplasts. *Biochim. Biophys. Acta.* 40:257–272.
12. Farkas, D. L., and S. Malkin. 1979. Cold storage of isolated class C chloroplasts. Optimal conditions for stabilization of photosynthetic activities. *Plant Physiol.* 64:942–947.
13. Arnold, W. A., and R. J. Azzi. 1977. Two effects of electrical fields on chloroplasts. *Plant Physiol.* 60:449–451.
14. Barber, J., and S. Malkin. 1981. Salt-induced microscopic changes in chlorophyll fluorescence distribution in the thylakoid membrane. *Biochim. Biophys. Acta.* 634:344–349.
15. Malkin, S., and B. Kok. 1966. Fluorescence induction studies in isolated chloroplasts. I. Number of components involved in the reaction and quantum yields. *Biochim. Biophys. Acta.* 126:413–432.
16. Herzenberg, L. A., R. G. Sweet, L. A. Herzenberg. 1976. Fluorescence activated cell sorting. *Sci. Am.* 234:108–117.
17. Farkas, D. L., R. Korenstein, and S. Malkin. 1982. Ionophore-mediated ion transfer in a biological membrane: a study by electrophotoluminescence. *In* Transport in Biomembranes. Model systems and Reconstitution. R. Antolini, A. Gliozzi, and A. Gorio, editors. Raven Press, New York. 215–226.
18. Schlodder, E., and H. T. Witt. 1980. Electrochromic absorption changes of a chloroplast suspension induced by an external electric field. *FEBS (Fed. Eur. Biochem. Soc.) Lett.* 112:105–113.
19. Zimmerman, U., G. Pilwat, F. Riemann. 1974. Dielectric breakdown of cell membranes. *Biophys. J.* 14:881–899.
20. Witt, H. T. 1975. Primary acts of energy conservation in the functional membrane of photosynthesis. *In* Bioenergetics of Photosynthesis. Govindjee, editor. Academic Press, Inc., New York. 493–554.
21. Pauly, H., L. Packer, and H. P. Schwan. 1960. Electrical properties of mitochondrial membranes. *J. Biophys. Biochem. Cytol.* 7:589–601.
22. Schwan, H. P. 1963. Determination of biological impedances. *In* Physical Techniques in Biological Research. W. L. Wastuk, editor. Academic Press, Inc., New York. 6:323–407.
23. Cole, K. S. 1970. Dielectric properties of living membranes. *In* Physical Principles of Biological Membranes. F. Snell, J. Wolken, G. Iverson, and J. Lam editors. Gordon & Breach, Science Publishers, Inc., New York. 1–16.
24. Hope, A. B. 1956. The electric properties of plant cell membrane. I. The electric capacitance of suspensions of mitochondria, chloroplasts and *Chlorella sp. Aust. J. Biol. Sci.* 9:53–66.
25. Packham, N. K., J. A. Berriman, and J. B. Jackson. 1978. The charging capacity of the chromatophore membrane. *FEBS (Fed. Eur. Biochem. Soc.) Lett.* 89:205–210.
26. De Grooth, B. G., H. J. van Gorkom, and R. F. Meiburg. 1980. Electrochromic absorbance changes in spinach chloroplasts induced by an external electrical field. *Biochim. Biophys. Acta.* 589:299–314.
27. De Grooth, B. G., H. J. van Gorkom, and R. F. Meiburg. 1980. Generation of the 518 nm absorbance change in chloroplasts by an externally applied electrical field. *FEBS (Fed. Eur. Biochem. Soc.) Lett.* 113:21–24.